UNIVERSITY OF MISKOLC
FACULTY OF MECHANICAL ENGINEERING AND INFORMATICS

ENHANCING SOLAR EFFICIENCY: NUMERICAL SIMULATION AND OPTIMIZATION OF THE TEMPERATURE-DEPENDENT POWER OUTPUT

Booklet of PhD Theses

PREPARED BY:

Husniddin Khayrullaev

Electrical Engineering , Electro Mechanics and Electrical Technologies (BSc)
Electrical Mechanic (by branches) a specialization (MSc)

ISTVÁN SÁLYI DOCTORAL SCHOOL OF MECHANICAL ENGINEERING SCIENCES
TOPIC FIELD OF BASIC ENGINEERING SCIENCES
TOPIC GROUP OF TRANSPORT PROCESSES AND MACHINES

HEAD OF DOCTORAL SCHOOL

Dr. Gabriella Bognár
DSc, Full Professor

HEAD OF TOPIC GROUP

Prof. Dr. László Baranyi
CSc, Full Professor

SCIENTIFIC SUPERVISOR

Dr. Endre Kovács

PhD, Associate Professor

Miskolc
2026

JUDGING COMMITTEE

Chair:

Secretary:

Members:

OFFICIAL REVIEWERS

1. INTRODUCTION

Fickian diffusion, or Fourier-type heat conduction, is one of the most fundamental processes for mass or energy transport. In the simplest case, it can be described by a single linear partial differential equation (PDE) in space and time:

$$\frac{\partial u(x,t)}{\partial t} = \alpha \frac{\partial^2 u(x,t)}{\partial x^2} + q\,, \tag{1.1}$$

where $x,\ t,\ \in \mathbb{R}, u = u(x,t)$ is the concentration (temperature in case of heat conduction) as a function of space and time, $\alpha = k/(c\rho)$ is the thermal diffusivity, where $c = c(\vec{r},t), \rho = \rho(\vec{r},t)$, $k = k(\vec{r},t)$ are the specific heat, the density and the heat conductivity of the material, respectively. Here, q is the heat generation or source term. Generalisations of this equation, including the advection-diffusion equation and several types of advection-diffusion-reaction equations [1], can simulate particle movement and propagation in physical, chemical, and biological systems [2]. Similar PDEs are used to simulate fluid flow through porous media, including moisture, ground water [3,4].

If the conductivity depends on space, then, instead of dealing with the $\alpha \cdot \partial^2 u(x,t)/\partial x^2$ phrase in one space dimension, I have to deal with the term

$$\frac{1}{c(x)\rho(x)} \frac{\partial}{\partial x}\left(k(x) \frac{\partial u}{\partial x} \right). \tag{1.2}$$

One can use a more general form instead of (1.1), valid in arbitrary space dimensions:

$$\frac{\partial u}{\partial t} = \frac{\nabla(k \nabla u)}{c\rho} + q\,,$$

where ∇ is the Nabla differential vector operator, $\nabla = \vec{i}\left(\partial/\partial x\right) + \vec{j}\left(\partial/\partial y\right) + \vec{k}\left(\partial/\partial z\right)$.

Many numerical approaches have been developed to solve Equation (1.1) and its generalisations. Most of them belong to the broad family of finite difference schemes (FDM) [5,6], which frequently indicates a form of method of lines [1]. The spatial variables are discretised first to generate an ordinary differential equation (ODE) system, and then an ODE solver is applied.

Fisher's equation, commonly known as the Fisher-Kolmogorov-Petrovsky-Piskunov equation [7], adds an additional logistic reaction term to the usual diffusion term:

$$\frac{\partial u}{\partial t} = \alpha \nabla^2 u + \beta u(1-u)\,. \tag{1.3}$$

Here, u is the unknown function and β is a non-negative parameter. In this case, the range of u is the unit interval $[0, 1]$. The equation is the conventional heat equation without the logistic element, where u is the temperature, which is frequently expressed in Kelvin units. The spread of gene variations in space, the growth and distribution of misfolded proteins in neuro-physiology [8], and the propagation of fronts in combustion processes [9] are all modelled by Eq. (1.3). Some chemotaxis models [10], can be considered as further generalization of Fisher's equation.

Huxley's equation [11] is considered in the following form:

$$\frac{\partial u}{\partial t} = \alpha \nabla^2 u + \beta u^2 (1-u) \tag{1.4}$$

where α and β are nonnegative real numbers. Solutions of the diffusion or heat equation satisfy the minimum and maximum principles. [12]. The minimum principle guarantees that the equation does not produce negative values if the initial and boundary values are non-negative, which is called the positivity-preserving property. When there is a reaction or other source term in the equation, these criteria are not always applicable.

Systems of diffusion-reaction equations are among the most widespread partial differential equations (PDEs) in science and technology. Therefore, analytical solutions are sought and found not only in the old times [13], but recently as well. For example, Simpson et al. [14] constructed analytical solutions of coupled linear reaction–diffusion equations where the space domain is growing in time. Escorcia and Suazo [15] very recently showed how to construct solutions in explicit form via similarity transformations and a Ricatti-system for coupled reaction-diffusion equations where the coefficients depends on time.

In recent years, concerns over climate change and rising heating energy demands have driven research toward more energy-efficient buildings, for example by optimizing insulation strategies [16]. Reducing energy consumption in buildings can be achieved through multiple approaches, including improvements in facade materials. For instance, studies suggest that stone cladding is more effective in minimizing cooling loads compared to aluminium composite panels, plaster, or polyurethane board systems [17]. Investments in energy efficiency become more financially viable as energy prices increase, yet studies show that consumer response to rising energy costs remains relatively inelastic in the short term.

The global transition to sustainable energy has established solar photovoltaics (PV) as a cornerstone technology. The importance of renewables like solar power stems from their clean nature, declining costs, and long-term viability, evidenced by a rapid deployment that has led to a global installed capacity exceeding 2 Terawatts (TW) [77]. While the primary focus of PV research has often been on improving the electrical conversion efficiency of semiconductor materials, the operational temperature of the panel is a paramount factor that directly impacts this efficiency.

In my research, I worked with my supervisor on investigating and improving families of novel and conventional explicit methods for solving linear and nonlinear heat conduction Fishers,

Huxley, Difussion equations, depending on a new way of thinking. Adapt the most successful methods (especially the Leapfrog-hopscotch and the original hopscotch methods) to cases where there is heat transfer by convection and (Stefan-Boltzmann-type, thus nonlinear) radiation, especially the problems of real-life heat transfer in buildings and Solar panel. The aim of this thesis is twofold: first, to develop and analyze explicit numerical methods for a class of time-dependent PDEs under a novel theoretical approach; and second, to extend the most robust of these methods especially the Leapfrog-Hopscotch method to handle coupled convective and radiative boundary conditions. This extension enables the high-fidelity simulation of practical engineering problems, specifically the complex heat transfer processes occurring in building envelopes and photovoltaic solar panels.

For the purposes of establishing the primary discretization framework in this chapter, I will consider the homogeneous case where this source term is absent, i.e., q=0 Eq (1.1).

In the case of Eq. (1.1) in one space dimension, I apply to the $\alpha\nabla^2 u$ term the most common central difference equation

$$\frac{\partial^2}{\partial x^2}u(x_i) \approx \frac{\frac{u(x_{i+1})-u(x_i)}{\Delta x}+\frac{u(x_{i-1})-u(x_i)}{\Delta x}}{\Delta x} = \frac{u_{i-1}-2u_i+u_{i+1}}{\Delta x^2}\ , \qquad (1.5)$$

which is second order in Δx, where $i=1,...,N-1$ and N is the overall number of nodes. Applying this process leads to the following spatially discretized formulation in one dimension:

$$\frac{du_i}{dt} = \alpha\frac{u_{i-1}-2u_i+u_{i+1}}{\Delta x^2}\ . \qquad (1.6)$$

Now let us give the discretisation of the heat transfer equation under the assumption that the parameters α, k, c, and ρ, which describe the properties of materials, are functions of space rather than fixed values Eq. (1.2).

In this example, the heat conduction equation can be discretised as follows:

$$c(x_i)\rho(x_i)\left.\frac{\partial u}{\partial t}\right|_{x_i} = \frac{1}{\Delta x}\left[k\left(x_i+\frac{\Delta x}{2}\right)\frac{u(x_i+\Delta x)-u(x_i)}{\Delta x}+k\left(x_i-\frac{\Delta x}{2}\right)\frac{u(x_i-\Delta x)-u(x_i)}{\Delta x}\right].$$

The nodes are surrounded by cells, and $k_{i,i+1}$ is the heat conductivity between node i and its right neighbour. The discretized equation attains the following form:

$$\frac{du_i}{dt} = \frac{1}{c_i\rho_i\Delta x}\left(k_{i,i+1}\frac{u_{i+1}-u_i}{\Delta x}+k_{i-1,i}\frac{u_{i-1}-u_i}{\Delta x}\right)\ . \qquad (1.7)$$

A cell's dimensions, measured along its length and across its (typical) cross-section, are denoted by Δx and S. Here u_i is the temperature of the cell i, $C_i = c_i\rho_i V$ is the heat capacity of that cell in $[\mathrm{J/K}]$ units, and $V = S\Delta x$ is the volume of the cell.

2. METHODOLOGY OF THE STUDY

My goal is to adapt and optimize numerical methods to efficiently investigate heat transfer in building walls and solar panels, enabling thermodynamic and economic optimization of building envelopes. I studied explicit positivity-preserving methods for heat equations with space- and time-dependent diffusion, assessing their accuracy, stability, and efficiency for stiff problems. I developed numerical methods for Fisher's equation by combining hopscotch and leapfrog techniques, testing their performance on small/large and stiff/non-stiff systems. I investigates dynamically consistent methods for Huxley's equation using operator-splitting, comparing computational efficiency via running-time measurements. I applies eight unconditionally stable explicit methods to coupled reaction-diffusion equations, showing they outperform standard approaches for low/medium precision. I uses transient simulation to assess heat loss through walls in five cold cities over six months, determining optimal insulation thickness for energy and cost efficiency. I presents a 1D heat conduction model for a PV panel with internal heat generation and convective-radiative boundaries, solved via the leapfrog-hopscotch method, revealing thermal gradients and time lag through the panel.

2.1 Some Explicit Methods

2.1.1 The Original odd-even hopscotch (OOEH) method

The original odd-even hopscotch (OOEH) method [18] a classic example of the explicit methods which is stable for the linear diffusion equation. It requires a special spatial structure. In essence, the mesh must be divided into two parts, the so called odd and even nodes (or cells), where the closest neighbour of the even cells are odd and vice versa. First, the FTCS formula is applied to the odd cells, followed by the BTCS (Backward-time Central-space) formula, which is based on implicit Euler time discretisation. After every time step, the odd and even labels are switched, as it is illustrated in Figure 2.1. The equations being used are as follows:

$$\text{First stage: } u_i^{n+1} = u_i^n(1-r) + r\left(u_{i-1}^n + u_{i+1}^n\right). \tag{2.1}$$

$$\text{Second stage: } u_i^{n+1} = \frac{u_i^n + r\left(u_{i-1}^n + u_{i+1}^n\right)}{1+r}. \tag{2.2}$$

2.1.2 The Leapfrog–Hopscotch (LH) method

The recently invented leapfrog hopscotch (LH) approach [19] also requires the odd-even space structure. Moreover, it has a structure made up of many full-time steps and two half time steps. Using the initial values, the calculation begins by taking a half-sized time step for the odd nodes. Full-time steps are then taken strictly alternately for the even and odd nodes until the last timestep

is reached, which should be halved for odd nodes to reach the same final time point as the even nodes, as shown in Figure 2.1. Since the first stage's time step is halved, the following general formula is applied:

$$u_i^{1/2} = \frac{u_i^0 + r\left(u_{i-1}^0 + u_{i+1}^0\right)/2}{1+r/2} \quad . \tag{2.3}$$

Next, for the even nodes, a full-time step is made using

$$u_i^1 = \frac{u_i^0(1-r/2) + r\left(u_{i-1}^{1/2} + u_{i+1}^{1/2}\right)}{1+r/2} \quad . \tag{2.4}$$

Full time steps in the same manner are then taken for the odd and even nodes in turn. Lastly, the computations for the odd nodes must be closed using a half-length time step.

$$u_i^1 = \frac{u_i^0(1-r/2) + r\left(u_{i-1}^{1/2} + u_{i+1}^{1/2}\right)}{1+r/2} \quad . \tag{2.5}$$

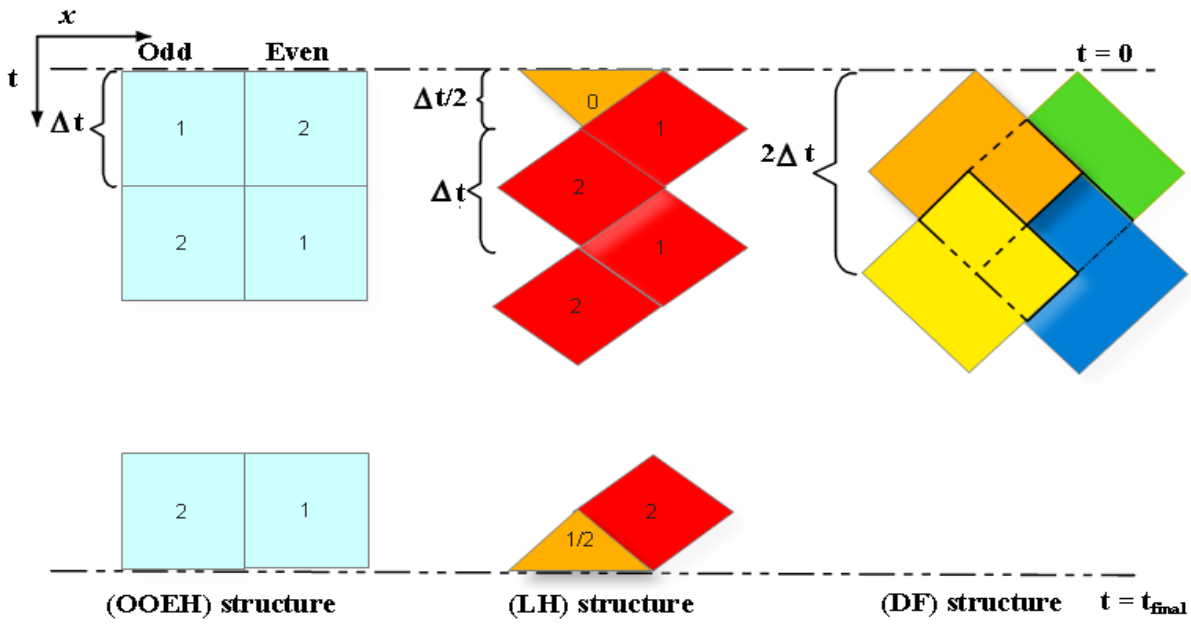

Figure 2.1. The structures of original odd-even hopscotch (OOEH), of leapfrog-hopscotch (LH) and Dufort–Frankel (DF) methods.

2.1.3 The Dufort–Frankel (DF) algorithm

This method can be obtained from the so called leapfrog explicit scheme by a modification [20] (p. 313). It is a known explicit unconditionally stable scheme that has the formula in the special and general case:

$$u_i^{n+1} = \frac{(1-2r)u_i^{n-1} + 2r\left(u_{i-1}^n + u_{i+1}^n\right)}{1+2r} \quad \text{and} \quad u_i^{n+1} = \frac{(1-r_i)u_i^{n-1} + 2A_i}{1+r_i} \quad . \tag{2.6}$$

As one can see, it is a one-stage but two-step method (the formula contains u_i^{n-1}), which is not self-starter, so another method must be applied to start the method by the calculation u_i^1. For this purpose, we apply the UPFD formula twice (with halved time step size).

2.2 A thorough investigation of explicit, positivity-preserving methods for the heat equation

I investigate the performance of 12 explicit non-conventional algorithms. All of them have the convex combination property; therefore, they are unconditionally stable and preserve the positivity of the solution when applied to the heat equation.

Now $N_x = 91$, $N_y = 100$, and $t_{\text{fin}} = 0.2$. The initial condition is $u_i^0 = rand$ to ensure that short and long-wavelengths components are present. The distribution of the capacities and the resistances has a width of six order of magnitude: $a_C = a_{Rx} = a_{Ry} = 3$, $b_C = b_{Rx} = b_{Ry} = 6$. This yields a very large stiffness and low CFL limit: thus $SR = 1.17 \cdot 10^{11}$ and $h_{MAX}^{FTCS} = 1.4 \cdot 10^{-6}$.

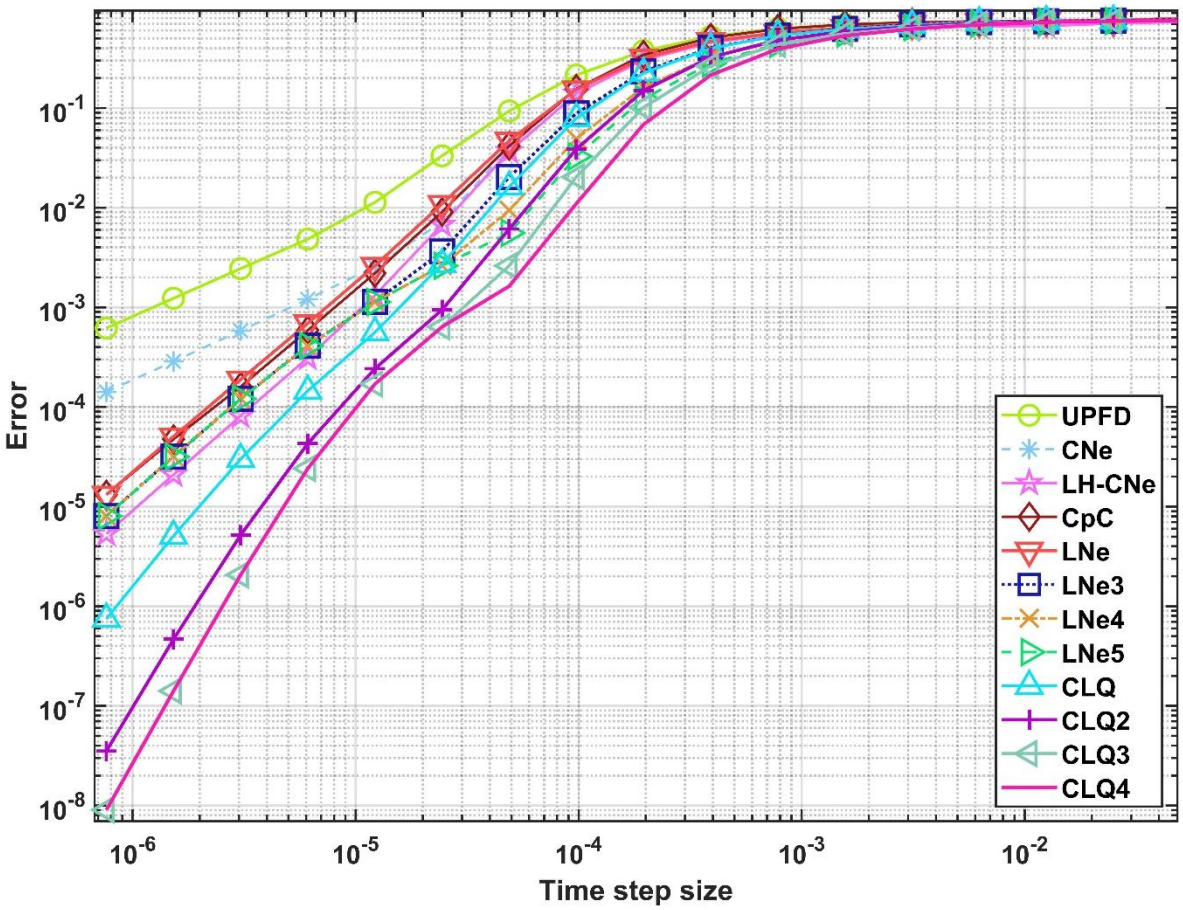

Figure 2.2. The error as a function of time step size Δt for very stifff system.

Since the system is quite large, the fluctuations in the running times are relatively low. The result of this numerical experiment is presented in Fig 2.2.

2.3 *Explicit, dynamical consistent methods for Fisher's equation*

I present new numerical approaches for solving Fisher's equation, which comprises both a linear diffusion term and a nonlinear logistic term. The conventional explicit finite difference techniques are only conditionally stable for this equation, and even when stable, they can provide concentrations that are less than zero or more than one. I compiled a list of algorithms here which are not only stable and explicit but possess the convex combination property for the diffusion equation. Based on these, I construct All of them are unconditionally dynamically consistent with Fisher's equation, so the concentration remains in the unit interval for any parameter. I thoroughly examine the performance of numerical schemes by performing tests in the case of 1D systems to explore how the errors depend on the coefficient of the nonlinear term, the stiffness ratio, and the anisotropy of the system. The analytical solution [21], valid for $\alpha = 1$:

$$u^{\text{exact}}(x,t) = \left(1 + e^{\sqrt{\frac{\beta}{6}}x - \frac{5}{6}\beta t} \right)^{-2}, \tag{2.7}$$

is used as reference solution of PDE (1.3). The initial condition is obtained simply by substituting the initial time into Eq. (2.7). The appropriate Dirichlet boundary conditions are prescribed by substitution of the left and right-side coordinate of the examined interval, which is $x \in [0, 2]$. The initial and the final times are $t^0 = 0$ and $t^{\text{fin}} = 0.1$. This is discretized

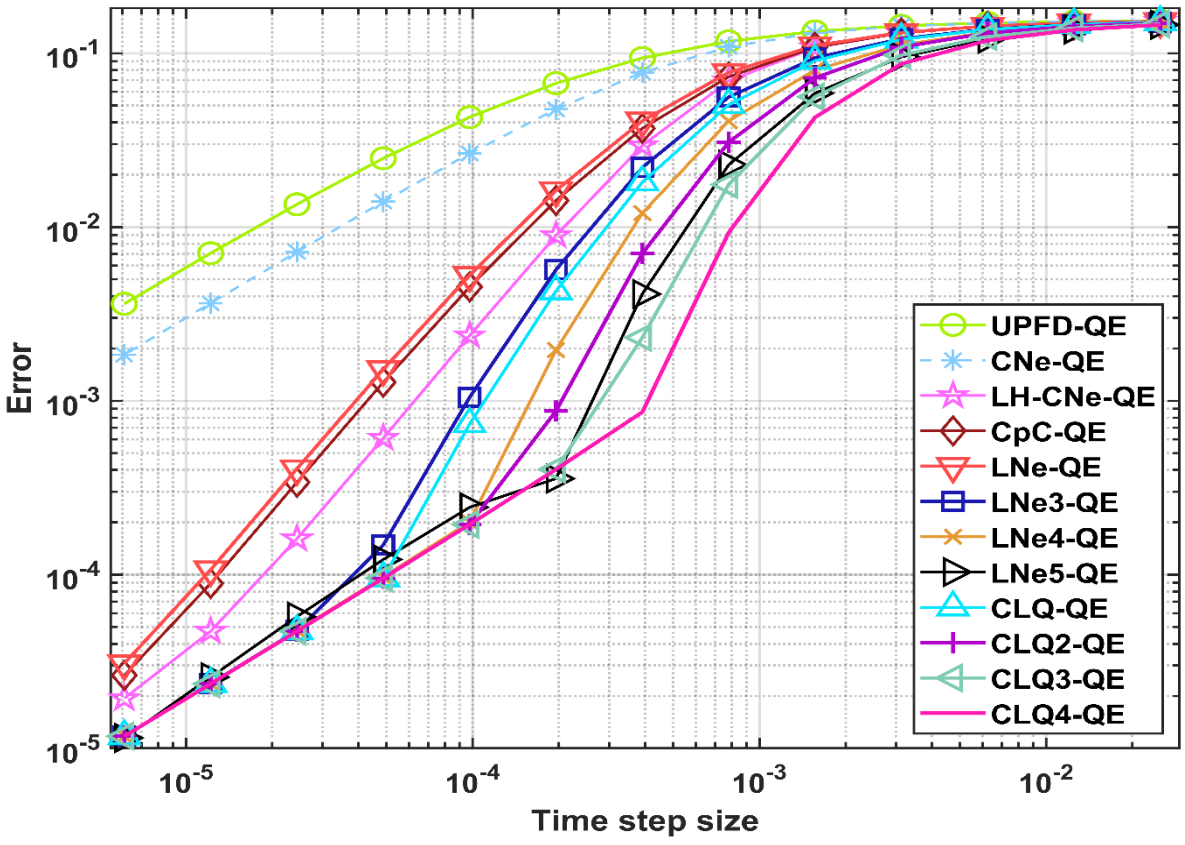

Figure 2.3. Maximum errors as a function of the time step size for QE treatment.

$x_j = x_0 + j\Delta x$, $j = 1,...,100$, $\Delta x = 0.02$ by dividing it into 100 equal parts . The nonlinear coefficient is quite large, $\beta = 29$. In my experiments, I calculated the error for S=13 different time step sizes for all the examined methods. The results for three different kinds of treatment are presented in Fig 2.3. Very similar plots have been obtained for the three other treatments and for other values of parameters β, t^{fin}, etc. The algorithms exhibit smooth convergence and show no signs of instability. However, as noted above, the inconsistent terms in the truncation error cause this convergence to be slow for larger time step sizes. The algorithms exhibit smooth convergence and show no signs of instability

2.4 Dynamically consistent methods for Huxley's equation

The efficiency of various numerical methods for solving Huxley's equation which includes a diffusion term and a nonlinear reaction term is investigated. Conventional explicit finite difference algorithms often suffer from severe stability limitations and can yield unphysical concentration

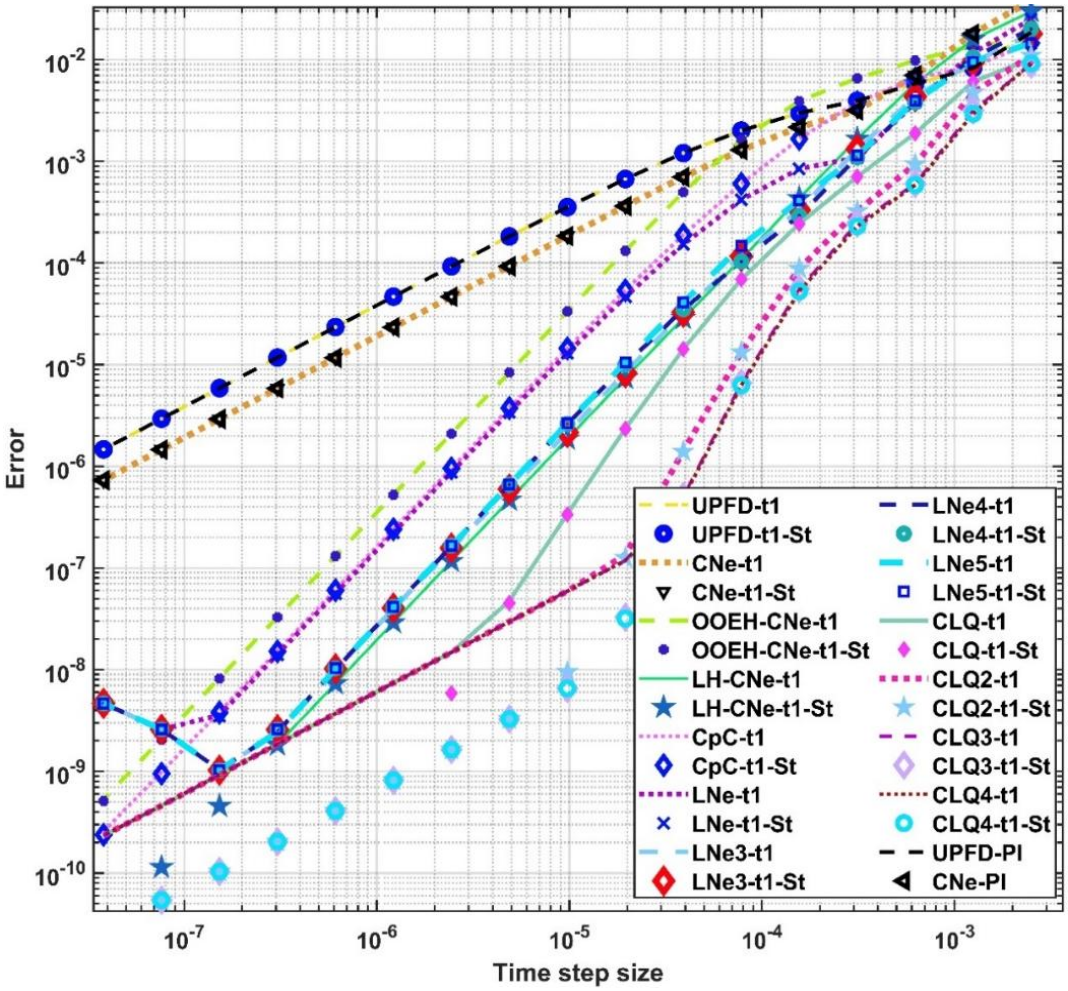

Figure 2.4. Maximum errors as a function of the time step size in stiff system.

values. I collect a range of stable, explicit time integration methods of first to fourth order, originally developed for the diffusion equation, and design treatments of the nonlinear term that ensure that the solution remains within the physically meaningful unit interval. This property,

called dynamical consistency, is analytically proven and implies unconditional stability. In addition to this, the most effective ones are identified from the large number of constructed method combinations. I conduct systematic tests in one and two spatial dimensions, also evaluating computational efficiency in terms of CPU time. Our results show that higher-order schemes are not always the most efficient: in certain parameter regimes, second-order methods can outperform their higher-order counterparts.

The stiff system with weaker nonlinearity figure 2.4 size is $N_x = 51, N_y = 60,$ the final time is $t^{\text{fin}} = 0.01$ the coefficient of the reaction-term $\beta = 2.9,$ while the exponents are $a_C = 3, b_C = 6, a_{Rx} = 1, b_{Rx} = 2, a_{Ry} = 2, b_{Ry} = 4$. The problem we obtained using these parameters is characterized by the $SR = 2.68 \cdot 10^9$ and $h_{MAX}^{FTCS} = 2.1 \cdot 10^{-5}$ numbers, hence the system is rather stiff. The initial concentration-function is smooth: $u_i^0 = \frac{1}{\sqrt{1+i}} + 0.001$.

2.5.1 *Solution of Huxley's equation by efficient numerical methods*

Thus, in this subsection, I start from those four explicit and stable numerical schemes. Using these diffusion solvers, several new methods are constructed for the nonlinear Huxley equation.

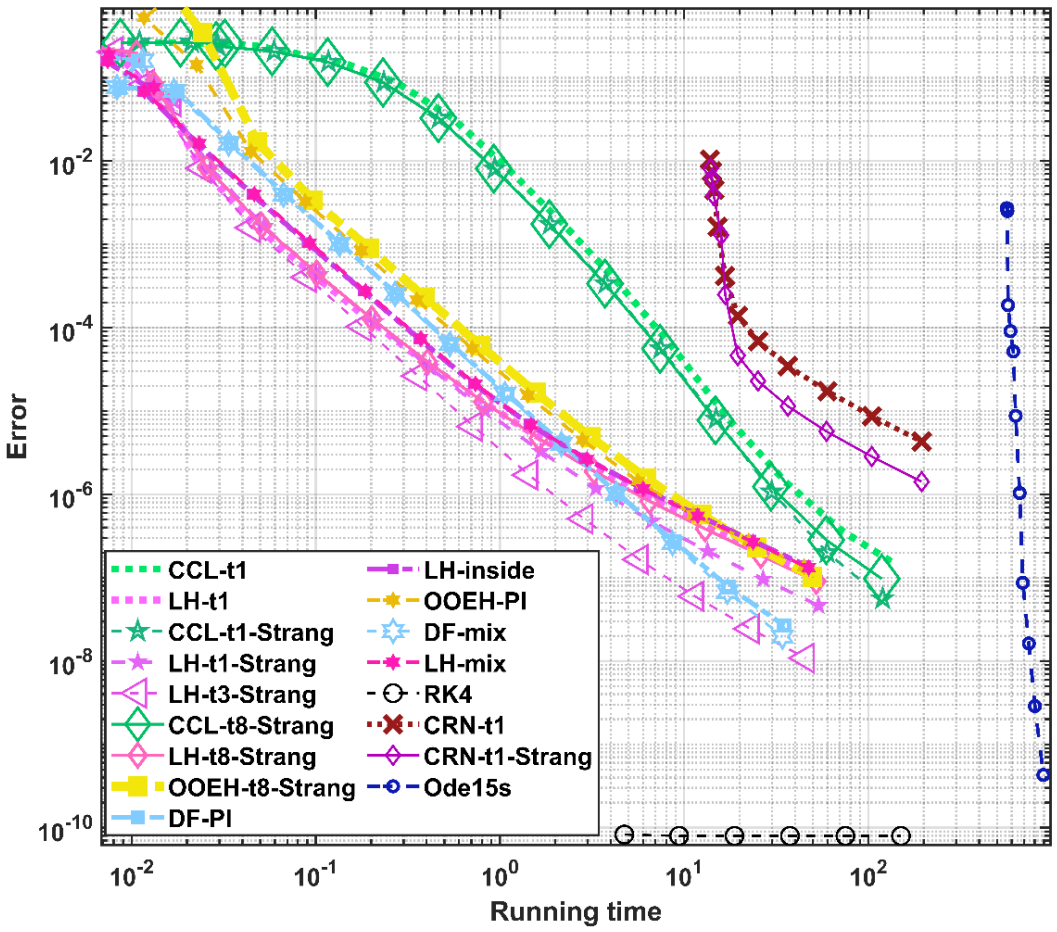

Figure 2.5. Maximum errors as a function of the running time moderately stiff system.

Then, based on extensive numerical case studies in two-dimensional spatial domains, the least-performing methods are gradually eliminated, leaving only the best-performing ones. During the tests, as above, not only a single time-step size but all relevant time-step sizes are considered, and corresponding run-time measurements are performed. Moderately stiff system fig-2.5, while the exponents are $a_C = a_{Rx} = a_{Ry} = 0, b_C = b_{Rx} = b_{Ry} = 2$ the system size and the final time used are $N_x = 101, N_y = 120, t^{\text{fin}} = 0.1$, and $\beta = 21$, These variables give $SR = 8 \cdot 10^5$ and $h_{MAX}^{FTCS} = 7.73 \cdot 10^{-5}$. This indicates that the system is moderately stiff only. The initial concentrations contain random numbers in the unit interval as follows:

$$u_i^0 = 0.3 cos\left(\frac{x}{N_x}\frac{\pi}{2}\right) cos\left(\frac{y}{N_y}\frac{\pi}{2}\right) + 0.6 rand \cdot$$

2.6 *Solution of coupled system of two reaction-diffusion equations*

Fig. 2.6, I display the errors calculated as a function of the time step size for both u and w for each method. I consider the verification successful, since for decreasing Δt, the errors are decreasing as expected based on our similar experiments conducted for single diffusion-type equations. I note that the FTCS and the AB2 methods produce meaningful solutions only below $\Delta t = 10^{-5}$ (bottom left corner of the figure).

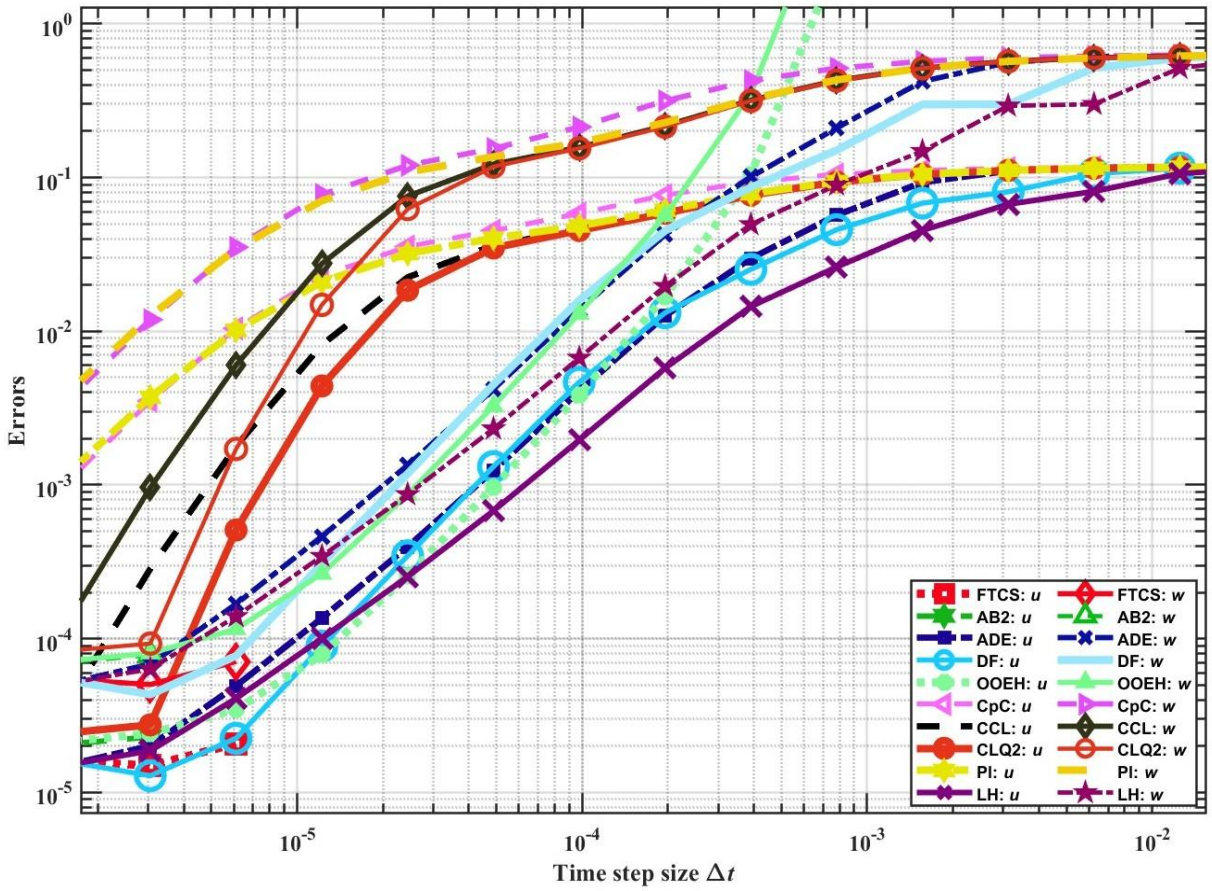

Figure 2.6. L2 errors as a function of the time step size Δt the simple coupling case.

2.6 Impact of climate variability on optimal thickness of wall insulation: a numerical study across five cold cities using long-term numerical simulations

All transient simulations were performed using a constant time step of Δt =50 s. The simulated time interval is from 15 of October to 15 of April, with duration T=184×24×3600=15894000 s, and it represents the whole heating season in most cities. It follows that there are always NT=$T/\Delta t$=317880-time steps in total. The weather data was obtained hourly from the website over the whole 2023–2024 winter season [101]. After then, linear interpolation was used to compute the data every 50 s. The studied cities Warsaw, Hokkaido, Edmonton, Ulaanbaatar, and Copenhagen are characterized by continental climates (Köppen D-type). Warsaw, Hokkaido, Edmonton, and Copenhagen have a humid continental climate with warm summers (Dfb), whereas Ulaanbaatar exhibits a subarctic climate with dry winters (Dwc). Key meteorological conditions in mid-January, including average outdoor temperature, solar radiation, and wind speed, strongly influence building heat loss and insulation performance. Table 7.1 summarizes these parameters, which were used as boundary conditions in the transient simulations. Understanding these climatic factors helps optimize insulation thickness and energy savings in cold climates.

Table 2.1. Mid-January Climatic Conditions and Köppen Classification of the Studied Cities.

City	Köppen Climate	Avg. Temp (°C)	Solar Radiation (W/m²)	Wind Speed (m/s)
Copenhagen	Dfb	0.0	90	4.0
Edmonton	Dfb	-10.0	120	5.0
Hokkaido	Dfb	-6.5	130	4.2
Ulaanbaatar	Dwc	-20.1	150	5.5
Warsaw	Dfb	-3.2	110	3.5

In this investigation, the true material properties listed in Table 7.2 are taken into account. Although these coefficients have a discontinuity at the material's boundary, they are constants inside the material and do not vary with temperature, time, or space.

Table 2.2. Properties of the materials used in the simulation

Material	$c\left[\mathrm{Jkg^{-1}K^{-1}}\right]$	$\rho\left[\mathrm{kgm^{-3}}\right]$	$k\left[\mathrm{Wm^{-1}K^{-1}}\right]$
Gypsum plaster	977	805	0.29
Panels	800	1600	0.743
Glass wool	700	120	0.039

Figure 2.7 illustrates the total heat loss (in W/m²) over time for a two-layer south-facing wall without insulation in five different cold cities. Ulaanbaatar (dashed black line) exhibits the highest average heat loss, peaking above 120 W/m², indicating a harsh winter climate with extreme temperature variations. Overall, the figure highlights the impact of climate conditions on heat loss

through an uninsulated south-facing wall. Cities with more extreme winter temperatures, such as

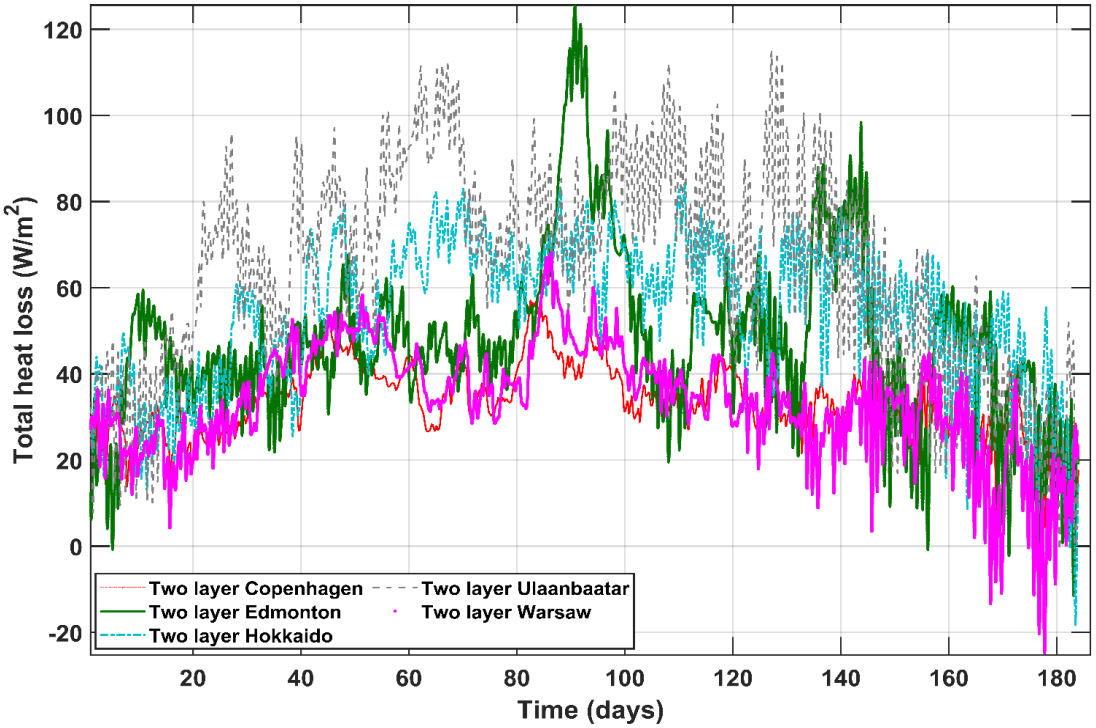

Figure 2.7. The heat loss in W units as a function of time in days for the simulation of the five cities for the south wall without insulation.

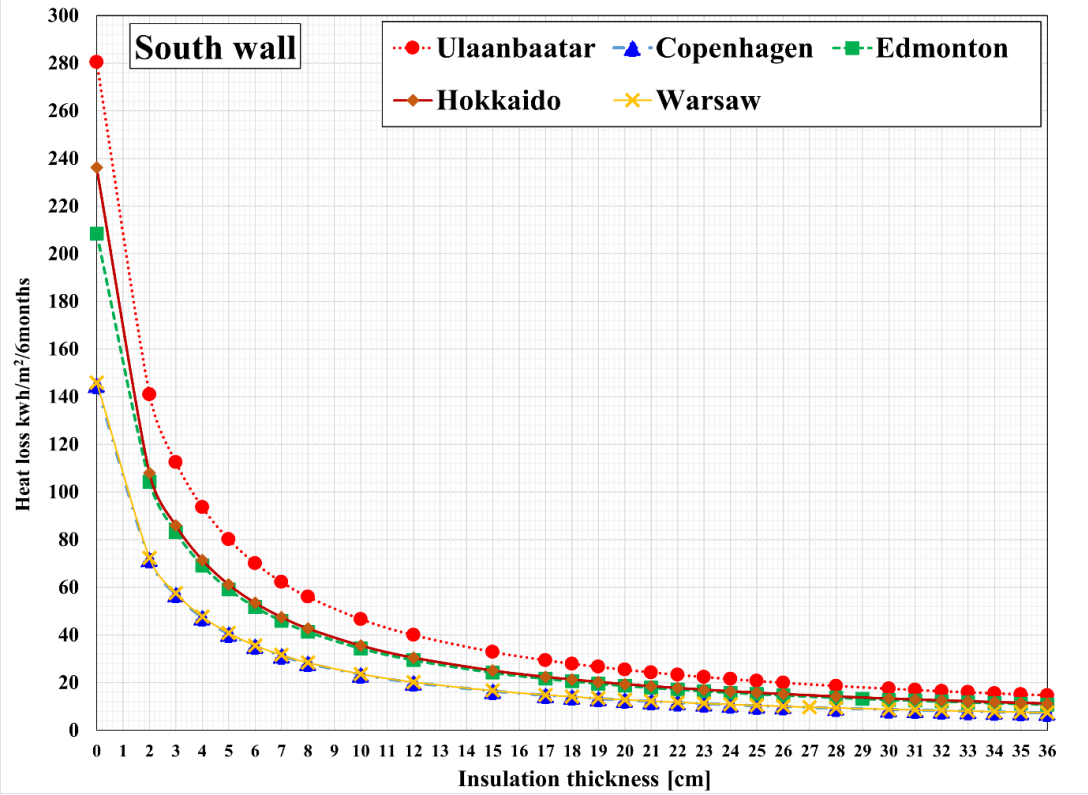

Figure 2.8. The heat loss in kWh/m^2/6 months as a function of insulation thickness of the south wall for the five cities

Figure 2.8 illustrates the heat loss as a function of insulation thickness of the south wall for the five cities. We can see all cities show a large decrease in heat loss as insulation thickness increases. Design strategies for energy efficiency must consider climate-specific requirements, as colder regions benefit more from thicker insulation. Adding insulation to the south wall is highly effective up to a point, especially in colder cities such as Ulaanbaatar.

2.8 Transient thermal simulation of a multi-layer photovoltaic panel using the leapfrog-hopscotch method

I present a detailed transient thermal analysis of a representative five-layer solar panel structure consisting of a glass front sheet, two ethylene–vinyl acetate (EVA) encapsulant layers, a silicon cell layer, and an aluminum back sheet. The thermal behaviour of the photovoltaic (PV) module is described using a one-dimensional heat transfer model that includes heat conduction, light absorption, and convective and radiative heat exchange with the surrounding environment. I assumed that the PV module operates under standard test conditions (STC), which in practice means using standard reference data for ambient temperature $u_a = 25°C$. An incident solar irradiance of 800 W/m² is applied to the top surface of the panel and is incorporated into the heat source term.

The transient thermal response of the PV panel, simulated over a two-hour period with a computational time step of $\Delta t = 10$ seconds, is shown in Figure 2.9.

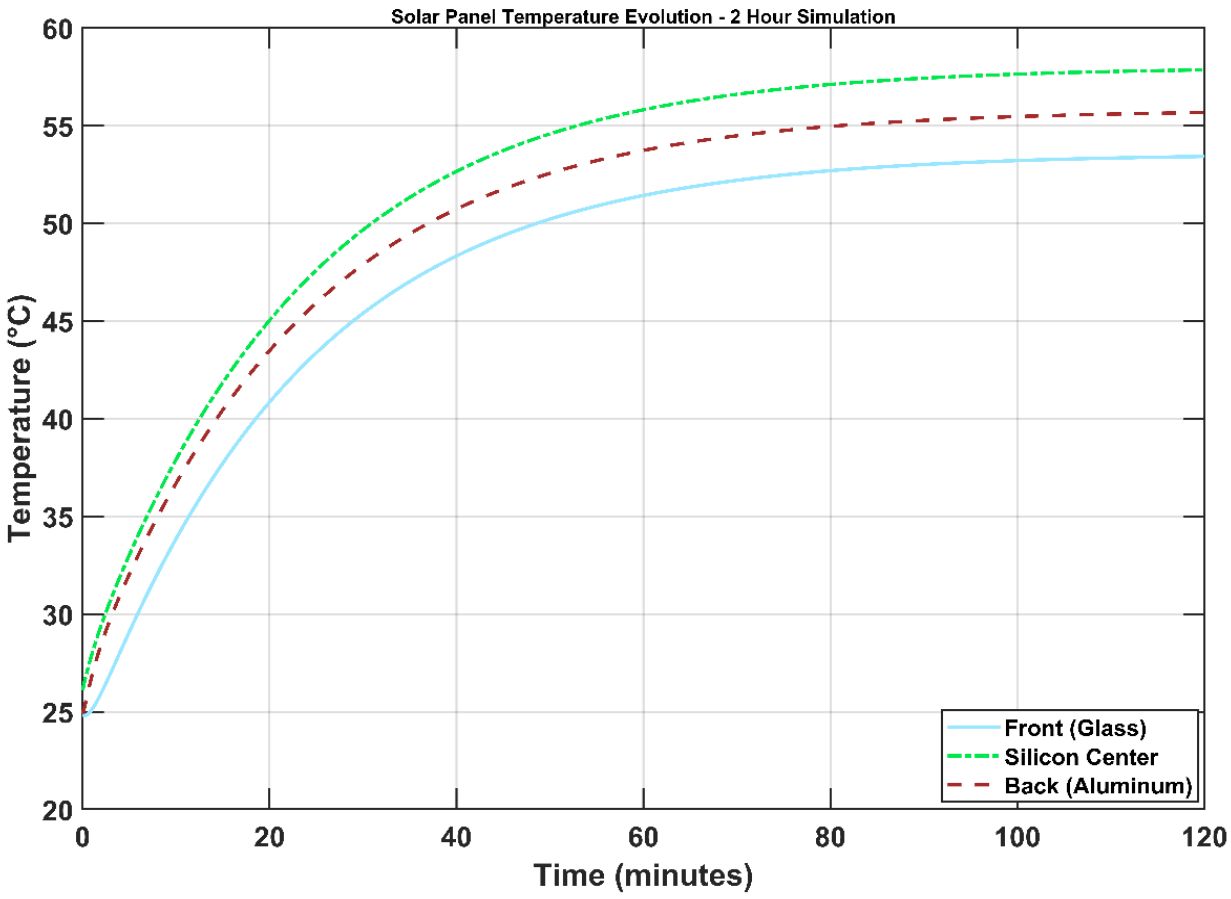

Figure 2.9. The temperature of the PV panel as a function of time in minutes.

3. NEW SCIENTIFIC RESULTS – THESES

T1. I examined several numerical algorithms possessing the convex combination property for the heat conduction equation. The methods accurately reproduced the analytical reference solution in one space dimension and the numerical reference solution in two space dimensions. As the stiffness parameter increased, the differences in accuracy between the methods decreased, indicating the presence of order reduction. This finding suggests that higher-order methods provide clear advantages mainly for non-stiff or moderately stiff problems, while lower-order schemes can be sufficiently efficient for very stiff cases. The tests confirmed expectations based on previous analytical results, namely that all examined methods satisfying the maximum–minimum principle remained stable over a wide range of time step sizes, including highly stiff regimes. Among them, LH-CNe proved to be the most efficient for low to medium accuracy requirements. When high accuracy is needed, higher-order CLQ methods are preferable, and multi-stage LNe methods can achieve comparable accuracy for smooth initial conditions (8),(10).

T2. I systematically investigated explicit numerical algorithms for Fisher's equation that are unconditionally dynamically consistent, i.e. keep the solution in the unit interval as the original equation does. I combined twelve diffusion schemes with pseudo-implicit and quasi-exact treatments of the nonlinear logistic term, including Strang-splitting, yielding 72 algorithm combinations. Through comprehensive numerical testing in one- and two-dimensional systems with exact reference solutions and stiff, anisotropic random media, I evaluated the accuracy, stability, and computational efficiency of the method. Based on aggregated error measures and running time analysis, I identified the ten most effective methods and demonstrated that quasi-exact treatments combined with higher-order CLQ schemes and Strang-splitting provide superior accuracy for strong nonlinearity, while simpler LH-CNe-based methods are optimal for low-accuracy or weakly stiff problems (7).

T3. I solved the nonlinear Huxley equation, whose true solution remains within the unit interval, using numerous algorithm combinations with operator-splitting. I employed methods which preserve this unit-interval property for arbitrary spatial meshes, time steps, and nonlinear coefficient β. Through numerical experiments, I identified the most effective schemes under different conditions. I recommend the LH-CNe solver with t1 treatments and Strang-splitting when speed is prioritized, stiffness is moderate, or β is large, while the CLQ family is preferable for high accuracy in stiff problems. I also found that Strang-splitting is unnecessary for very small nonlinear coefficient. For complicated geometries, the CpC-t1-Strang solver offers high speed with acceptable accuracy (5).

T4. I performed extensive numerical tests to solve Huxley's equation, focusing on the most efficient methods with proven unconditional stability for the linear diffusion equation. I found that the LH solver with t1 treatment and Strang-splitting is generally the most efficient and reliable, providing accurate results quickly even for extremely stiff systems with strong nonlinearity. For complicated geometries where odd-even cell division is difficult, the CCL-t1-Strang or DF-mixed methods proved to be reliable alternatives, while the original odd-even hopscotch method is suitable only for equidistant meshes with constant diffusion parameters. The Crank-Nicolson method is computationally expensive for large systems and offers no clear advantage over LH, though standard Newton iterations may improve accuracy for small systems. For extreme accuracy requirements, higher-order methods such as RK4 perform better than low-order schemes (6).

T5. I analyzed a coupled system of two reaction–diffusion equations with time-dependent reaction terms and used analytical solutions involving Kummer functions as reference solutions. I applied eight explicit numerical methods with excellent stability properties and verified their performance using the analytical solutions. By extensive parameter-sweep experiments, I demonstrated that these methods substantially outperform standard explicit schemes, and that the leapfrog–hopscotch method is generally the most efficient for solving such coupled systems (4).

T6. I developed a transient numerical framework to investigate the impact of climate variability on the optimal insulation thickness of building walls using long-term simulations driven by real meteorological data. By extending the heat conduction equation to include convection, radiation, and solar heat gains and solving it with the explicit leapfrog–hopscotch method, I simulated heat transfer through multilayer walls for five cold-climate cities with different Köppen classifications. I demonstrated that the leapfrog–hopscotch method enables stable and accurate simulations over an entire heating season using time steps far beyond the CFL limits of standard explicit schemes. Using life-cycle economic analysis, I identified climate-specific optimal insulation thicknesses and showed that colder cities benefit from significantly thicker insulation, while solar gains on south-facing walls reduce the economically optimal thickness in milder climates. The results confirm that optimal insulation design must account for both climatic severity and wall orientation, and that long-term transient simulations provide more realistic guidance than steady-state approaches (2).

T7. I developed a transient one-dimensional thermal model for a multilayer photovoltaic panel incorporating incoing sunshine and electric energy production in the form of positive and negative internal heat generation, respectively, radiative and convective boundary conditions, and realistic material properties. The governing heat conduction equation was discretized using a finite difference approach and solved with the explicit leapfrog–hopscotch method, demonstrating computational efficiency. Numerical simulations revealed persistent thermal gradients across the panel thickness, with the silicon cell acting as the dominant thermal hotspot. These results provide a reliable numerical framework for evaluating photovoltaic thermal behaviour and optimizing thermal management and module design (3).

4. LIST OF PUBLICATIONS RELATED TO THE TOPIC OF THE RESEARCH FIELD

(1) Khayrullaev, H., Omle, I., & Kovács, E. (2026). Prediction of heat transfer in building walls of different materials using neural networks and finite difference methods. *Eng, 7*(4), Article 173. https://doi.org/10.3390/eng7040173.

(2) Khayrullaev, H., Zain, A., Omle, I., & Kovács, E. (2026). Impact of climate variability on optimal thickness of wall insulation: A numerical study across five cold cities using long-term numerical simulations. *Applications in Engineering Science, 25*, Article 100294. https://doi.org/10.1016/j.apples.2026.100294.

(3) Khayrullaev, H. Transient thermal simulation of a multi-layer photovoltaic panel using the leapfrog-hopscotch method. Conference Paper Dec. 2025.

(4) Khayrullaev, H., Zain, A., & Kovács, E. (2025). Solution of coupled systems of reaction–diffusion equations using explicit numerical methods with outstanding stability properties. *Computation, 13*(6), Article 129. https://doi.org/10.3390/computation13060129.

(5) Khayrullaev, H., & Kovács, E. (2025). Unconditionally dynamically consistent numerical methods with operator-splitting for a reaction–diffusion equation of Huxley's type. *Mathematics, 13*(17), Article 2848. https://doi.org/10.3390/math13172848.

(6) Khayrullaev, H., Omle, I., & Kovács, E. (2025). Exploring the performance of some efficient explicit numerical methods with good stability properties for Huxley's equation. *Mathematics, 13*(2), Article 207. https://doi.org/10.3390/math13020207.

(7) Khayrullaev, H., Omle, I., & Kovács, E. (2024).Systematic investigation of the explicit, dynamically consistent methods for Fisher's equation. *Computation, 12*(3), Article 49. https://doi.org/10.3390/computation12030049.

(8) Khayrullaev, H., & Kovács, E. (2024). Comprehensive investigation of the explicit, positivity preserving methods for the heat equation: Part 1. *Multidiszciplináris Tudományok, 14*(1), 46–59. https://doi.org/10.35925/j.multi.2024.1.5.

(9) Khayrullaev, H., & Kovács, E. (2024). Comprehensive investigation of the explicit, positivity preserving methods for the heat equation: Part 2. *Multidiszciplináris Tudományok, 14*(1), 60–70. https://doi.org/10.35925/j.multi.2024.1.6.

(10) Khayrullaev, H., & Kovács , E. (2024). Numerical performance of some positivity preserving methods for the diffusion equation where the diffusion coefficient depends on both time and space. *International Journal of Advanced Natural Sciences and Engineering Researches*, *8*(2), 284–292. Retrieved from https://as-proceeding.com/index.php/ijanser/article/view/1722

5. REFERENCES

[1] Hundsdorfer, W. H., & Verwer, J. G. (2003). *Numerical solution of time-dependent advection–diffusion–reaction equations*. Springer. https://doi.org/10.1007/978-3-662-09017-6

[2] Acton, Q.A. *Issues in Biophysics and Geophysics Research and Application: 2011 Edition*; ScholarlyEditions: Atlanta, GA, USA, 2012; ISBN 9781464964299.

[3] Zhokh, A., & Strizhak, P. (2022). Advection–diffusion in a porous medium with fractal geometry: Fractional transport and crossovers on time scales. *Meccanica, 57*, 833–843. https://doi.org/10.1007/s11012-021-01353-z.

[4] Yu, H., Yao, L., Ma, Y., Hou, Z., Tang, J., Wang, Y., & Ni, Y. (2022). The moisture diffusion equation for moisture absorption of multiphase symmetrical sandwich structures. *Mathematics, 10*(15), 2669. https://doi.org/10.3390/math10152669.

[5] Savović, S., & Djordjevich, A. (2008). Numerical solution of the diffusion equation describing the flow of radon through concrete. *Applied Radiation and Isotopes, 66*(4), 552–555. https://doi.org/10.1016/j.apradiso.2007.08.018.

[6] Suárez-Carreño, F., & Rosales-Romero, L. (2021). Convergency and stability of explicit and implicit schemes in the simulation of the heat equation. *Applied Sciences, 11*(10), 4468. https://doi.org/10.3390/app11104468.

[7] Li, Y., van Heijster, P., Marangell, R., & Simpson, M. J. (2020). Travelling wave solutions in a negative nonlinear diffusion–reaction model. *Journal of Mathematical Biology, 81*, 1495–1522. https://doi.org/10.1007/s00285-020-01547-1.

[8] Weickenmeier, J., Jucker, M., Goriely, A., & Kuhl, E. (2019). A physics-based model explains the prion-like features of neurodegeneration in Alzheimer's disease, Parkinson's disease, and amyotrophic lateral sclerosis. *Journal of the Mechanics and Physics of Solids, 124*, 264–281. https://doi.org/10.1016/j.jmps.2018.10.013.

[9] Campos, D., Llebot, J. E., & Fort, J. (2004). Reaction–diffusion pulses: A combustion model. *Journal of Physics A: Mathematical and General, 37*(26), 6609–6621. https://doi.org/10.1088/0305-4470/37/26/001.

[10] Columbu, A., Frassu, S., & Viglialoro, G. (2024). Refined criteria toward boundedness in an attraction–repulsion chemotaxis system with nonlinear productions. *Applicable Analysis, 103*(2), 415–431. https://doi.org/10.1080/00036811.2023.2187789

[11] Bradshaw-Hajek, B. (2009). *Reaction–diffusion equations for population genetics* [Doctoral dissertation, University of Wollongong]. UOW Research Online. https://hdl.handle.net/10779/uow.27833322.v1.

[12] Qin, X., Jiang, Z., & Yan, C. (2024). Strong stability preserving two-derivative two-step Runge–Kutta methods. Mathematics, 12(16), Article 2465. https://doi.org/10.3390/math12162465.

[13] Lienhard, J.H., IV; Lienhard, J.H., V. *A Heat Transfer Textbook*, 5th ed.; Phlogiston Press: Cambridge, MA, USA, 2017.

[14] Simpson, M. J., Sharp, J. A., Morrow, L. C., & Baker, R. E. (2015). Exact solutions of coupled multispecies linear reaction–diffusion equations on a uniformly growing domain. *PLoS ONE, 10*(9), Article e0138894. https://doi.org/10.1371/journal.pone.0138894.

[15] Escorcia, J.M.; Suazo, E. On explicit solutions for coupled reaction–diffusion and Burgers-type equations with variable coefficients through a Riccati system. *Discrete and Continuous Dynamical Systems – Series S* 2025.

[16] Abu Dabous, S., Ibrahim, T. E., Shareef, S., Mushtaha, E. S., & Alsyouf, I. (2022). Sustainable façade cladding selection for buildings in hot climates based on thermal performance and energy consumption. *Results in Engineering, 16*, Article 100643. https://doi.org/10.1016/j.rineng.2022.100643.

[17] Ghrab-Morcos, N. (2005). CHEOPS: A simplified tool for thermal assessment of Mediterranean residential buildings in hot and cold seasons. *Energy and Buildings, 37*(6), 651–662. https://doi.org/10.1016/j.enbuild.2004.09.020.

[18] Gourlay, A. R., & McGuire, G. R. (1971).General hopscotch algorithm for the numerical solution of partial differential equations. *IMA Journal of Applied Mathematics, 7*(2), 216–227. https://doi.org/10.1093/imamat/7.2.216.

[19] Nagy, Á., Omle, I., Kareem, H., Kovács, E., Barna, I. F., & Bognár, G. (2021). Stable, explicit, leapfrog–hopscotch algorithms for the diffusion equation. *Computation, 9*(8), Article 92. https://doi.org/10.3390/computation9080092.

[20] Hirsch, C. *Numerical Computation of Internal and External Flows, Volume 1: Fundamentals of Numerical Discretization*; Wiley: New York, NY, USA, 1988.

[21] Agbavon, K.M.; Appadu, A.R.; Khumalo, M. On the numerical solution of Fisher's equation with coefficient of diffusion term much smaller than coefficient of reaction term. *Advances in Difference Equations* 2019, 146.